



## Synthesis and characterization of new hybrid decatungstate anions (CTAB)<sub>4</sub>W<sub>10</sub>O<sub>32</sub>: Toward heterogeneous Photocatalysis

Samir Briche, El Mountassir El Mouchtari, Mustapha Boutamart, Oussama Jhabli, Lekbira El Mersly, Kaltoum Belkodia, Mohammed Amine Edaala, Pascal Wong-Wah-Chung, Otman Abida, Salah Rafqah

### ► To cite this version:

Samir Briche, El Mountassir El Mouchtari, Mustapha Boutamart, Oussama Jhabli, Lekbira El Mersly, et al.. Synthesis and characterization of new hybrid decatungstate anions (CTAB)<sub>4</sub>W<sub>10</sub>O<sub>32</sub>: Toward heterogeneous Photocatalysis. International Journal of Environmental Analytical Chemistry, In press, 10.1080/03067319.2023.2242267 . hal-04435878

**HAL Id: hal-04435878**

**<https://hal.science/hal-04435878>**

Submitted on 6 Feb 2024

**HAL** is a multi-disciplinary open access archive for the deposit and dissemination of scientific research documents, whether they are published or not. The documents may come from teaching and research institutions in France or abroad, or from public or private research centers.

L'archive ouverte pluridisciplinaire **HAL**, est destinée au dépôt et à la diffusion de documents scientifiques de niveau recherche, publiés ou non, émanant des établissements d'enseignement et de recherche français ou étrangers, des laboratoires publics ou privés.

# Synthesis and characterization of new hybrid decatungstate anions (CTAB)<sub>4</sub>W<sub>10</sub>O<sub>32</sub> : Toward heterogeneous Photocatalysis

Samir Briche<sup>a</sup>, El mountassir El mouchtari<sup>b,c</sup>, Mustapha Boutamart<sup>a</sup>, Oussama Jhabli<sup>a</sup>,  
Lekbira El Mersly<sup>b</sup>, Kaltoum Belkodia<sup>b</sup>, Mohammed Amine Edaala<sup>b</sup>, Pascal Wong-Wah-  
Chung<sup>c</sup>, Otman Abida<sup>d</sup>, Salah Rafqah<sup>b</sup>.

<sup>a</sup> Department of Energy Storage and Multifunctional Coatings, Moroccan Foundation for Advanced Science, Innovation and Research (M<sup>2</sup>AScIR), Rabat, Morocco.

<sup>b</sup> Laboratoire de Chimie Analytique et Moléculaire, Faculté polydisciplinaire de Safi, Université Cadi Ayyad, Morocco.

<sup>c</sup> Aix Marseille Université, CNRS, LCE, Marseille, France

<sup>d</sup> College of Engineering, American University of the Middle East, Egaila, Kuwait.

## Abstract:

In the present study, hybrid decatungstate based photocatalysts, [(C<sub>16</sub>H<sub>33</sub>)N(CH<sub>3</sub>)<sub>3</sub>]<sub>4</sub>[W<sub>10</sub>O<sub>32</sub>], were synthesized by the reaction of hexadecyltrimethylammonium surfactant (CTAB) and Na<sub>4</sub>W<sub>10</sub>O<sub>32</sub>·2.6H<sub>2</sub>O (W10), with different molar ratio W10:CTAB (1:1 for compound **1** and 1:3 for compound **2**). In order to verify that the materials have been formed, FTIR, UV-visible spectroscopy, TGA, XRD, and SEM tests were conducted. Comparing and analyzing the influences of molar ratios on band gap energy, photocatalytic activity, and material morphology is discussed. FTIR spectroscopy showed that CTAB reacted with W10 to produce an insoluble product in aqueous media. According to UV-visible spectroscopy, the hybrid material with a low amount of CTAB absorbs more light in the visible region than the other, with the optical band gap decreasing to 2.42 eV for compound **1**. After 7 hours of exposure, both compounds, compound **1** and **2**, demonstrated a 46 and 88% degradation of carbamazepine in aqueous solution using UV-visible photocatalysis.

**Keywords:** Hybrid decatungstate, heterogeneous photocatalysis, carbamazepine, water purification.

## 1. Introduction

Polyoxometalates (POMs) are metal-oxide species built from pseudo-octahedral MO<sub>6</sub> (M=V, Nb, Mo, W) units sharing corners and/or edge with the metal is in its higher oxidation degree.

Recently, POMs attracted a lot of attention for their promising proprieties in many application fields: catalysis and photocatalysis [1–6], biology [7] and medicine [8]. The POMs showed good redox reversibility, producing colored mixed-valence species while maintaining their structural integrity [9]. Among these POMs is decatungstate ion  $W_{10}O_{32}^{4-}$ , which is an isopolytungstate with a metal-oxide framework without any internal heteroatoms or heteroions. It has been widely used as a homogenous photocatalysts [10–12] for organic reactions and organic pollutant degradation in water [10,13–15], because of its interesting physical properties such as, high surface charge density and strongly basic oxygen surfaces. Otherwise, the research on isopolyacids is still limited, while most of the research papers in POMs area are focused on the heteropolyacids [16–18].

Research efforts have been concentrated on wastewater treatement using PMOs through advanced oxidation processes over the past few years. These materials can be used to replace conventional semi-conductors photocatalysts, which suffer from photo-corrosion and limited visible light absorption [19]. Moreover, in decatungstate system, the reactive species has a quite long lifetime ( $\tau_{wO}$  of  $65 \pm 5$  ns) [20] and are formed with a high quantum yield ( $\Phi_{wO}$  is 0.57). Nevertheless, decatungstate is highly soluble in aqueous solutions, which limits their potential application in heterogeneous photocatalysis, and consequently, heterogenization of decatungstate remains an appealing challenge for researchers. There are various strategies to incorporate decatungstate in solid support materials among them  $SiO_2$  [21–25],  $ZrO_2$  [26,27],  $TiO_2$  [28] and  $\gamma-Al_2O_3$  [29]. However, these composites revealed to be instable under irradiation and their activity limited due to the release of photoactive species in solution. Considering the very high photoactivity of decatungstate [30] it appeared sometimes difficult to attribute the observed efficiency to the heterogenous or homogeneous photocatalysis phenomenon. As result, solubility control was shown to be a key aspect of POM chemistry and application. The use of organic surfactant as hexadecyltrimethylammonium (CTAB) for POMs heterogenization was recently reported [31], and the hybrid materials obtained were structurally characterized without any application studies [32–34]. The CTAB cationic surfactant is very in water and environmentally friendly compounds, making it an ideal candidate for decatungstate heterogenization.

The aim of this work is to synthesize new water-insoluble heterogeneous decatungstate based photocatalysts, determine their structural properties and assess their photocatalytic activity through pollutant degradation. Carbamazepine (CBZ) was chosen as a pharmaceutical pollutant model for two reasons: (i) the use of classical dyes that are inappropriate for photocatalytic activity studies under visible light [35,36] (ii) CBZ in one of the most common pollutant

detected in wastewater and its elimination has been extensively studied [37–41], (iii) CBZ is almost photostable under visible light irradiation. Considering that the leaching of decatungstate is also one of our main concerns, we focused on a simple test that could be used as a standard one to test for hybrid materials based on decatungstate.

## **2. Experimental section**

### **2.1. Materials and Methods**

#### **2.1.1. Chemicals**

All Chemical reagents, hydrochloric acid (HCl; 37% purity), sodium chloride (NaCl; 99% purity), acetonitrile (CH<sub>3</sub>CN; 99.5% purity) and Hexadecyltrimethylammonium bromide (CTAB, 96% purity) were purchased from Sigma-Aldrich except sodium tungstate dihydrate (Na<sub>2</sub>WO<sub>4</sub>·2H<sub>2</sub>O, 99% purity) purchased from CARLO ERBA. All chemicals were used without further purification.

#### **2.1.2. Characterization equipment**

FTIR spectra were acquired in transmission mode in the 4000–400 cm<sup>-1</sup> spectral range using an ABB Bomem FTLA200 spectrometer and KBr pellet technique. Spectra of 16 scans were recorded in air atmosphere with a resolution of 16 cm<sup>-1</sup>. Thermogravimetric analysis (TGA) was performed under air atmosphere using TGA Q500 (TA 1000) equipment. The specimens (approximately 20 mg) were weighed in Platinum crucible. The samples were heated at a rate of 5°C.min<sup>-1</sup> from ambient temperature to 1000°C. The powder XRD data were collected on a Philips diffractometer, using Cu K $\alpha$  radiation from 5° to 80° (2 $\theta$ ) with 0.02° step. The UV-visible solid-state absorption spectra were recorded from a sample powder in quartz cell 1 mm-diameter on a Perkin Elmer Lambda 1050 UV/Visible/NIR instrument from 200 to 800 nm with 1 nm step and a 150 mm-diameter integrating sphere. The surface morphology of materials was analysed using High-resolution Scanning Electron Microscopy (SEM) with BRUKER-QUANTAX FEI instrument operated at 200 keV.

#### **2.1.3. Photocatalytic experiments**

The experiments were conducted with a LOT Quantum Xenon Lamp system (300 W) equipped with a 90° beam turner whose emission was filtered by a water and atmospheric filter (LOT Quantum Design LSZ231 and LSZ176) to deliver a wavelength ranged between 290–800 nm. A photocatalyst sample of 30 mg was suspended in 50 mL of an aqueous solution of Carbamazepine (CBZ) at 1×10<sup>-4</sup> mol.L<sup>-1</sup>. After 1 hour stirring in the dark at room temperature (25°C), the adsorption/desorption equilibrium was reached. The mixture was then placed in a

reactor (pyrex glass), and continuously stirred throughout the experiment. Mixture and reactor were kept at 20 °C by water flow [41].

#### 2.1.4. HPLC and LC MS analysis of CBZ

The concentration of **CBZ** was determined by liquid chromatography apparatus (UPLC PerkinElmer Altus 30) equipped with an Eclipse Plus C18 (3.5  $\mu$ m; 2.5  $\times$  150 mm) and a 220/240 pump, a 330-diode array UV-visible detector, a 363-fluorescence detector and a 410-automatic injector. An isocratic method was set at a flow rate of 0.25 mL.min<sup>-1</sup> and the injected volume was equal to 10  $\mu$ L. The separation was obtained using a 65:35 ratio of water/acetonitrile (with 0.1% formic acid) and the wavelength of absorption used for detection was 285 nm. Before injection, samples were systematically filtered on a 0.2  $\mu$ m cellulosic filter of 15 mm in diameter (Agilent Technologies) to remove the photocatalyst ensuring that CBZ was not retained on the filter.

Identification of carbamazepine degradation products was performed (LC-MS QTOF), using Agilent 1290. The source parameters were established as follows: fragmenter: 140 V, capillary voltage: 3000 V, skimmer 65 V, nebulizer pressure (30 psi), nebulizer needle voltage (500 V), nitrogen was used as desolvation gas (temperature 350°C, flow rate 10 L.min<sup>-1</sup>), and the flow rates for the sheath gas were set at 350°C and 8 L.min<sup>-1</sup> respectively.

### 2.2.Synthesis of materials

#### 2.2.1. Synthesis of Na<sub>4</sub>W<sub>10</sub>O<sub>32</sub>. xH<sub>2</sub>O

Na<sub>4</sub>W<sub>10</sub>O<sub>32</sub>.xH<sub>2</sub>O (**W10**) was prepared following literature procedures [42] with large modifications. First, a boiled aqueous solution of Na<sub>2</sub>WO<sub>4</sub>.2H<sub>2</sub>O (66 g in 400 mL) and HCl (1 M in 400 mL) were mixed for 20 seconds under strong stirring, then the mixture was cooled rapidly to 0°C. When the temperature has reached 30°C, an excess of NaCl salt was added to the mixture and at 0°C, a precipitate was formed. This precipitate was filtered and dried in vacuum and about 33 g of light-yellow solid were collected and placed for one night in freezer at -3°C. After dissolving the solid in hot acetonitrile (200 mL for 33 g of the solid formed), the solution was boiled for 2 to 3 minutes, and filtering was performed. A white solid residue containing predominantly sodium chloride was collected and the yellow-green solution (the filtrate) was evaporated at 25°C to obtain a yellow-green powder.

**2.2.2. Synthesis of [(C<sub>16</sub>H<sub>33</sub>)N(CH<sub>3</sub>)<sub>3</sub>]<sub>4</sub>[W<sub>10</sub>O<sub>32</sub>] hybrid materials.** A 20 mL of aqueous solution of decatungstate **W10** (2.44 g, 1 mmol) was added dropwise to 20 mL of aqueous solution of **CTAB** at different concentration (0.36 g (1 mmol) for **compound 1** and 1.08 g (3 mmol) for **compound 2**) under vigorous stirring. The mixture was refluxed at 100°C for 1 hour.

A pale-yellow precipitate was obtained for **compound 1**, and a white precipitate for **compound 2**. The precipitates were washed and filtered three-times with hot water and then dried overnight at 100°C.

### 3. Results and discussion

#### 3.1. Materials Characterization

To further establish the formation of hybrid materials, FT-IR spectral measurements were carried out. The representative results are shown in Figure 1. The FT-IR spectrum of **W10** shows the well-known absorptions bands of decatungstate [43,44]. The absorption band at 424.3  $\text{cm}^{-1}$  is assigned to W-O-W scissoring, the others at 578.6, 771.47, 833.18 and 902.62  $\text{cm}^{-1}$  are assigned to W-O<sub>corner-shard</sub>-W and W-O<sub>edge-shard</sub>-W stretching in the decatungstate framework, and the intense band at 964.33  $\text{cm}^{-1}$  is assigned to the stretching of W=O<sub>terminal</sub> [42,45–47]. Two bands are well resolved for the bending vibrations of water. The highest frequency band in the  $\delta(\text{HOH})$  vibrations range, at 1658  $\text{cm}^{-1}$ , corresponds to the weakly bonded waters, however the band at 1627  $\text{cm}^{-1}$  belongs to coordinated water molecules but with a weaker coordination bond [48]. A band was observed within 3500  $\text{cm}^{-1}$  for stretching vibrations of water  $\nu(\text{OH})$ , corresponding to coordinated water molecules. We carried out a thermogravimetric analysis to determine how many water molecules were chemisorbed and physisorbed. Thus, we counted about 2.6 structural water molecules in each cluster.

On the FT-IR spectrum of CTAB molecule the strong absorption at 2847, 2916 and 3016  $\text{cm}^{-1}$  respectively originated from C–H stretching vibration of methyl and methylene groups of CTAB. The absorption bands at 1481 and 1434  $\text{cm}^{-1}$  for pure hexadecyltrimethylammonium surfactant were due to the asymmetric and symmetric –C–H vibration of the quaternary ammonium group [44,49–51].

The FT-IR spectra of compounds **1** and **2** are similar with the characteristic's absorption bands of W10 and CTAB. This confirms that CTAB have successfully reacted with W10. The compounds **1** and **2** also bear the symmetric and asymmetric  $-(\text{CH}_2)-$  vibrations, which indicates the direct non-involvement of hydrocarbon chains in the reaction leading to the formation of compounds **1** and **2**. Additionally, the band at 1481  $\text{cm}^{-1}$  was broadened and shifted to 1465  $\text{cm}^{-1}$  and the peak at 1434  $\text{cm}^{-1}$  was not present, which suggest that hybrid materials influenced the quaternary ammonium group vibrations. In the stretching vibration

region at  $3448\text{ cm}^{-1}$ , a broad and less intense band was observed. This corresponds to adsorbed water molecules [52].

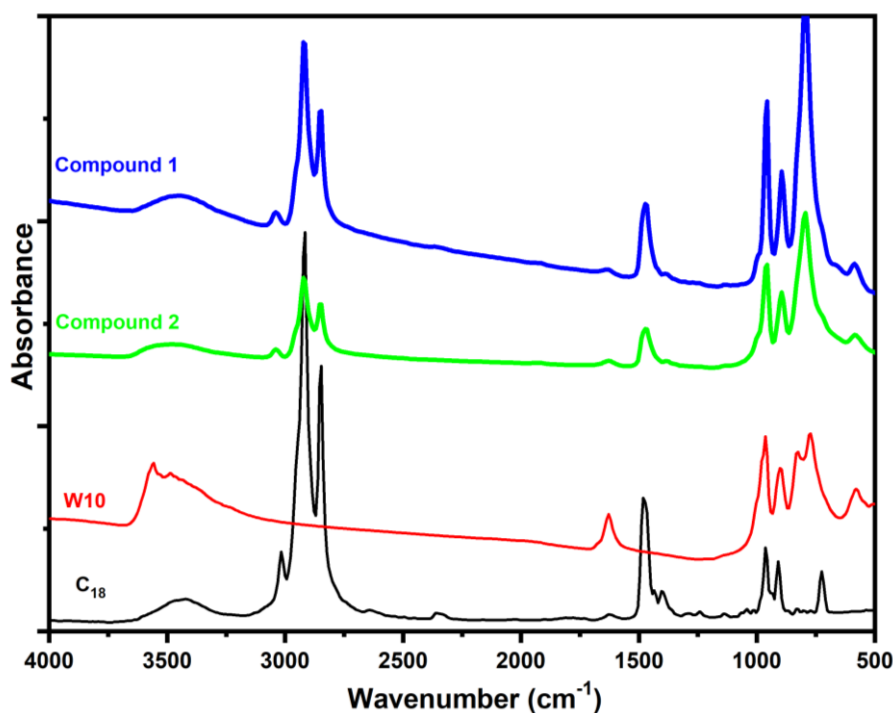


**Figure 1:** FT-IR spectra of W10, CTAB and hybrid materials (compound 1 and 2).

To investigate the thermal stability and establishing the chemical formula of compound **1** and **2**, a series of TGA experiments were carried out. The thermogravimetric analysis (figure 2), reveals that both compounds have almost similar thermal behaviour. Two main steps are observed in TGA for the decomposition process under air atmosphere. A first step ends at approximately  $375\text{ }^{\circ}\text{C}$ , and the second step is completed at approximately at  $500^{\circ}\text{C}$ . This represents a total weight loss of 34 and 31% for compound **1** and **2** respectively, which corresponds to the loss of 4 CTAB molecules.

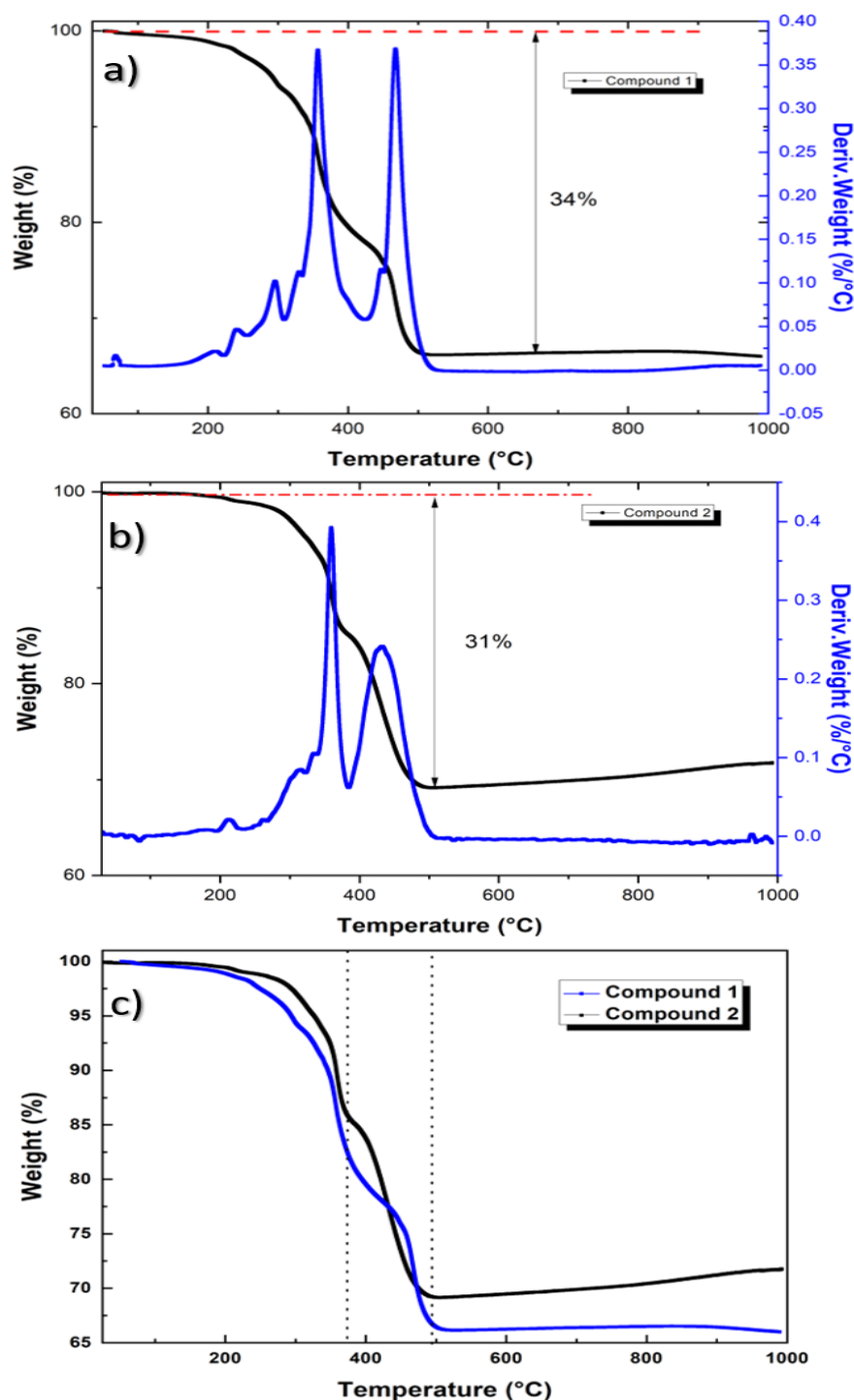


**Figure 2:** TGA curves of compound 1 (a) and compound 2 (b) and comparative curves (c).

Additionally, compound 2 decomposes at almost 50°C higher than the compound 1, which is a reliable indicator of its stability. The relatively high thermal stability of compound 2 ought to be attributed to the high crystallinity in comparison with compound 1 which is confirmed by XRD analysis in figure 3a. On the other hand, this temperature shift might be also due to encapsulation of CTAB ions, or strong interaction between CTAB and W10 [53,54]. In addition, it is important to note that the powder diffraction pattern (figure 3b) collected from a

solid's residue after TGA experiments for both compounds, confirms the formation of tungsten trioxide (WO<sub>3</sub>). Assuming the decomposition reaction (Eq.1), it can be shown that the observed weight loss nearly precisely corresponds to x:y ratio 4:10. Thus, the chemical composition of both compounds is (C<sub>19</sub>H<sub>42</sub>N)<sub>4</sub>W<sub>10</sub>O<sub>32</sub>.

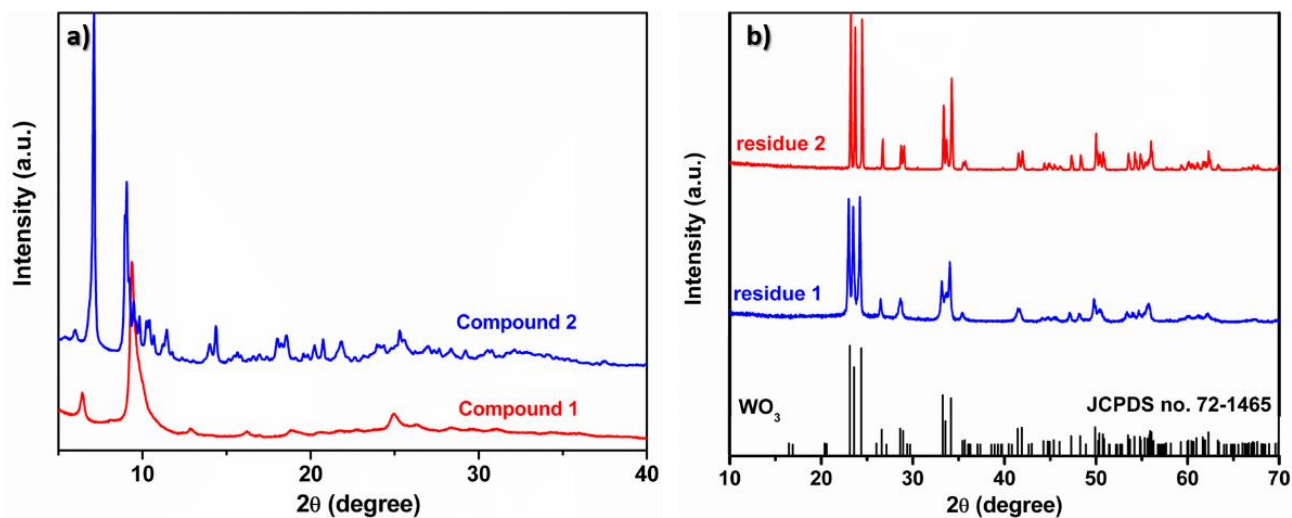
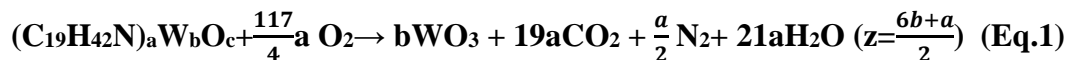


**Figure 3.** XRD patterns of (a) compound 1 and 2 and (b) TGA residues.

The morphology and microstructure of W10, compound 1 and 2 was investigated by scanning Electronic Microscopy (SEM). Figure 4.a shows images of W10, which is constituted by parallelepiped crystals of different sizes, the biggest ones having a 11×3×2.84 μm size. These parallelepiped crystals resulted from the aggregation of smaller building blocks of about 3.5×1 μm size.

The insertion of CTAB into the structure leads to morphological changes attested by the presence of edge-like aggregate with range size of 760-940 nm (Fig.4.b). With a higher concentration of CTAB (Fig.4.c), the structure is characterized by the discrete grains of layer particles with size in the range 6.61 to 8.5 μm. These observations suggest that the size and the morphology of the hybrid materials are different from W10, which indicates, that the use of CTAB molecules as a heterogenization agent give rise to a complete change in the morphology state of the hybrid materials. In fact, the shape and grain size of hybrid materials changed when the CTAB concentration was varied using water as reaction solvent. For compound 1, as the concentration of CTAB was close to the critical micelle concentration (CMC = 0,9 mmol in water), only a low amount of spherical CTAB micelles were formed leading to small size aggregates. On the contrary, with a 4 mM CTAB concentration, much more CTAB micelles are

formed and lead to lamellar phases. The aggregation reached  $6.84\ \mu\text{m}$ , with a distinct layered appearance. That indicates the formation of lamellar system which agrees with other study [55].

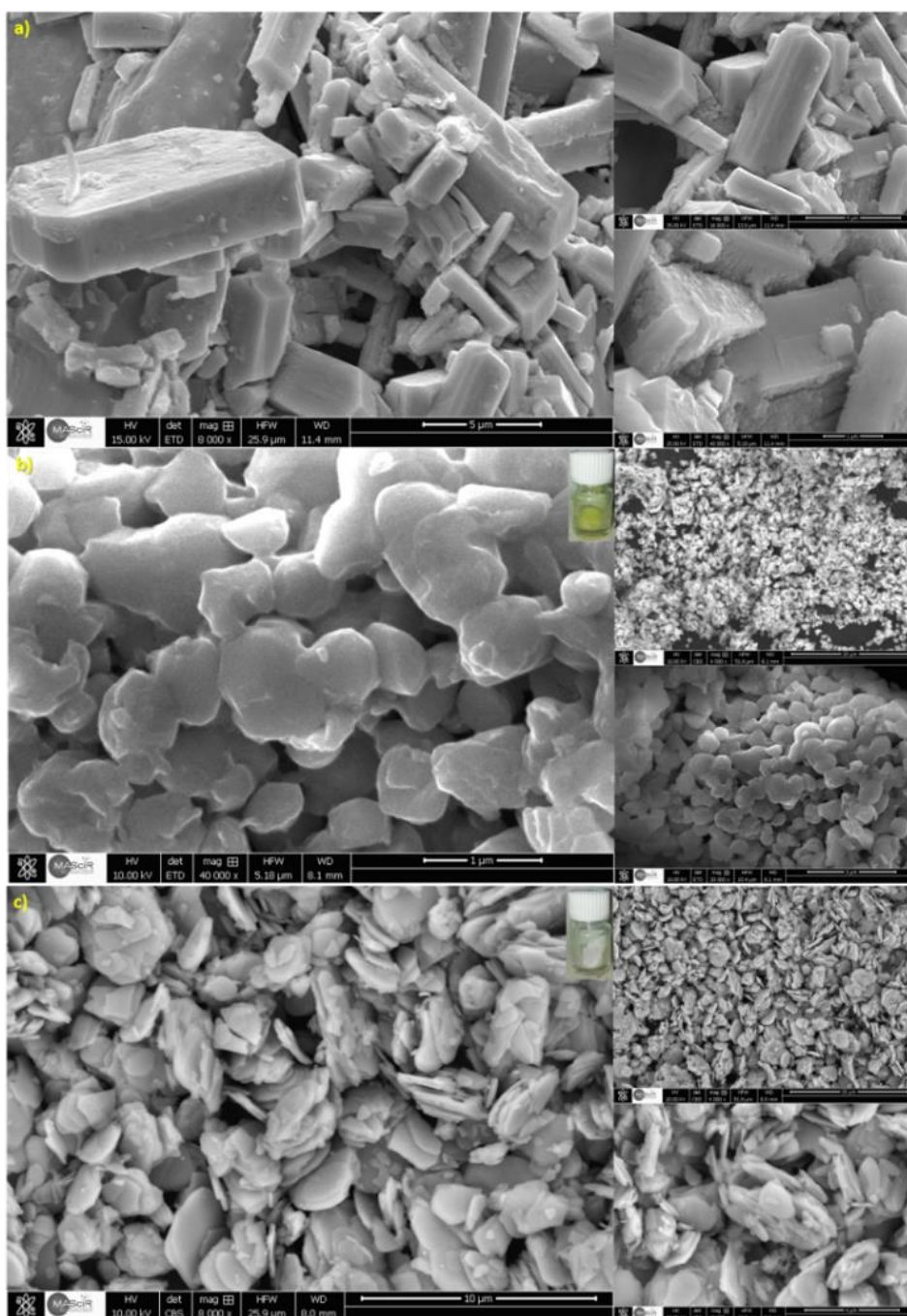


**Figure 4** SEM images of W10 (a), compound 1(b) and 2(c).

To understand the colour difference (green vs white) between the two hybrid compounds, their optical properties were investigated.

The UV-visible absorption spectra of W10, compound **1** and **2**, presented on figure 5.a., show a large absorption band in UV region. The maximum of absorption is located at 310 and 318

nm for W10 and compound **2**, respectively while for compound **1**, this band broadens in the visible region until 520 nm. The observed bands for the three compounds are typical to decatungstate [46] and are coming from HOMO-LUMO Transition Ligand to Metal Charge Transfer (LMCT) and more precisely to the bridging oxygen-to-tungsten charge transfer [56].

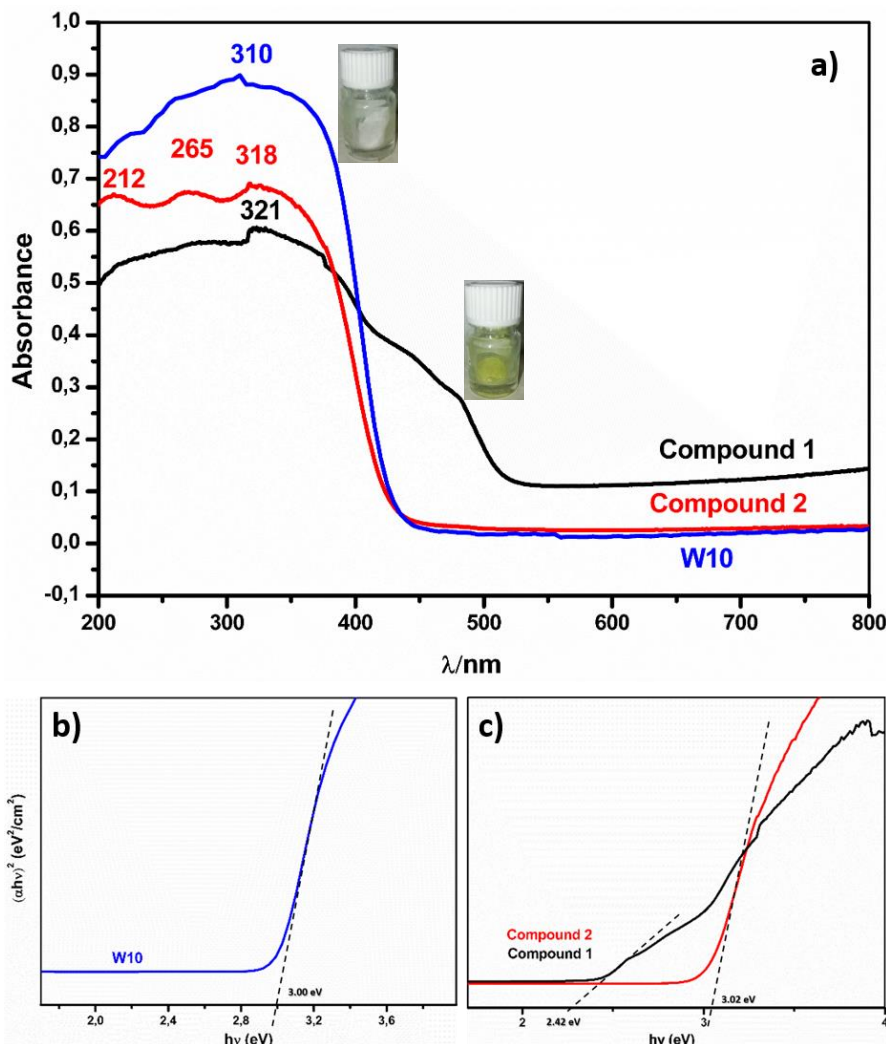


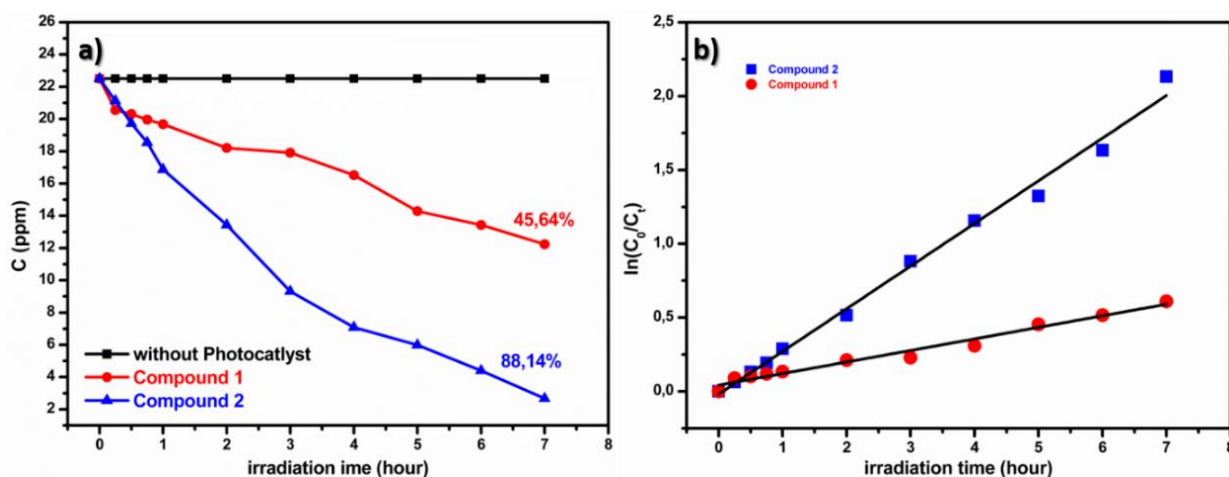
**Figure 5.** a) UV-Vis absorption spectra of W10, Compound 1 and 2. b) and c) K-M function vs energy (eV).

To estimate the optical band gap energy  $E_g$  (eV), UV-Visible spectrum was converted to Kubelka-Munk function  $\alpha h\nu = A(h\nu - E_g)^{n/2}$  and plotted against energy in eV (figure 5.b and 5.c), where  $\alpha$  is the absorption coefficient,  $\nu$  is the light frequency.  $A$  is a constant and  $n$  is the transition nature characteristic, which is estimated as a direct transition ( $n=1$ ). The band gap energy  $E_g$  can be defined as the intersection between the energy axis and the linear portion of the Kubelka-Munk function plot [19,57]. Thus, the band gap energy is equal to 3 eV for W10, 2.42 for compound **1** and 3.02 eV for compound **2**. These values suggest the promising optical proprieties of our hybrids for visible-light photocatalysis, especially compound **1**. This

demonstrates that the use of CTAB molecules as heterogenization agent allow the previous change in the morphology but also the modification of the optical gap energy.

## 2.2. Photocatalytic Study

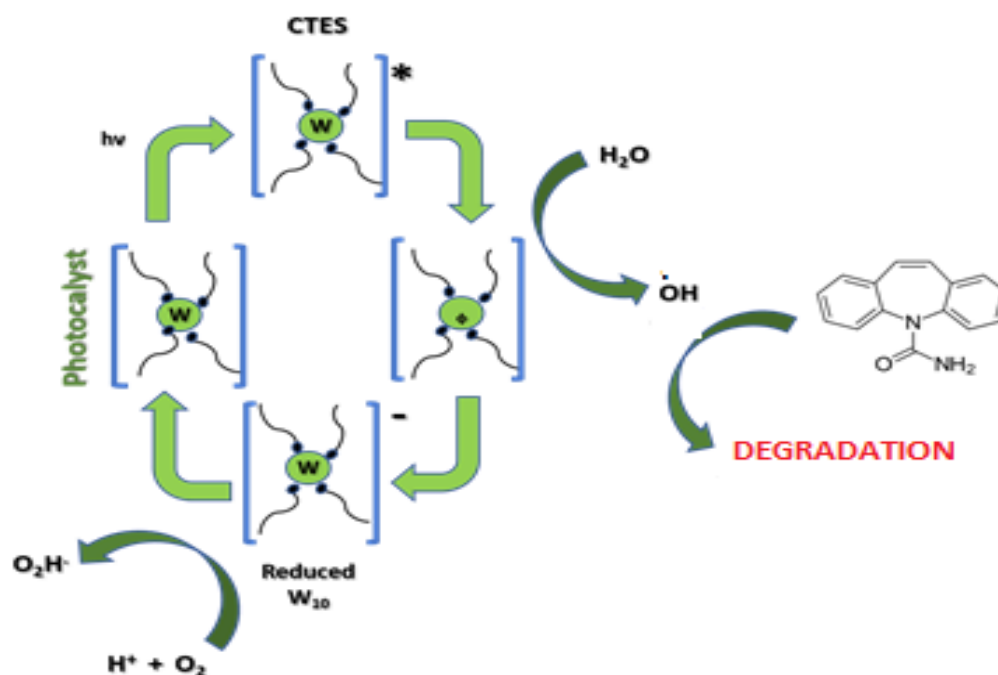
In order to evaluate the photocatalytic activities of compound **1** and **2**, a solution of CBZ ( $1 \times 10^{-4}$  mol L<sup>-1</sup>) was irradiated by UV-visible light from 300 W Xe Lamp in the absence and presence of the photocatalysts. It is worth noting that no direct photodegradation of CBZ is observed as shown in figure 6.a. On the other hand, in the presence of photocatalysts (30 mg), the degradation of CBZ were 45.65 and 88.14% after 7 hours of irradiation for compound **1** and **2** respectively (figure 6.a). The kinetics of CBZ photodegradation by compound **1** and **2** fit with pseudo-first-order equation as presented in figure 6.b. The apparent kinetic constants ( $k_{app}$ ) of **1** and **2** under UV-Visible light irradiation are  $7.83 \times 10^{-2}$  and  $2.89 \times 10^{-1} \text{ h}^{-1}$  respectively. The result indicates that despite the small optical gap energy of compound **1**, its efficiency was lower than compound **2** as observed previously by Zhao et al. for other hybrid polyoxometalates [58]. In fact, as the band gap of compound **1** is narrower than that of compound **2**, this is less favourable to charge separation [58]. Consequently, the production of free hydroxyl radicals is reduced and the induced photodegradation of organic compounds is decreased [59].



**Figure 3:** a) Concentration evolution of CBZ under UV irradiation without photocatalyst and with compound **1** and **2**. b) Kinetics equation of CBZ photodegradation by compound **1** and **2**.

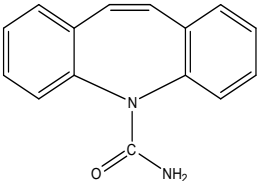
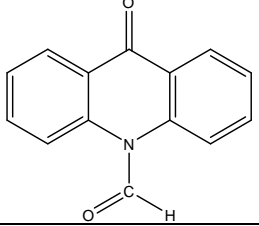
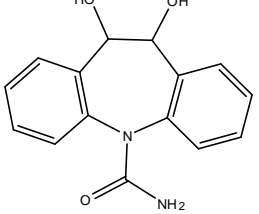
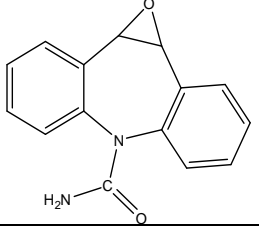
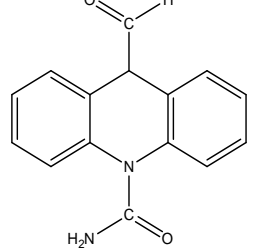
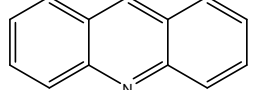
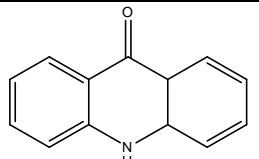
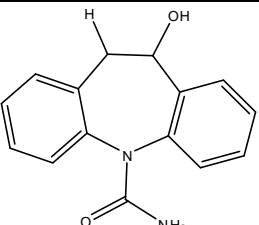
The hydroxyl radicals could be formed as follows: after absorption of photons, decatungstate is excited with the formation of a charge transfer excited-state ( $W_{10}O_4^{4-}$ )\*, which decays to a very reactive non-emissive transient species [60]. This species oxidizes water molecules to form

hydroxyl radicals ( $\bullet\text{OH}$ ) and a reduced decatungstate [61]. The reduced decatungstate being re-oxidized by  $\text{O}_2$  to form again decatungstate and peroxy radicals ( $\text{HO}_2\bullet$ ). This cycle is illustrated on figure 7, takes place continuously as long as the system is aerated and exposed to light. The formed free radicals, especially  $\bullet\text{OH}$ , can degrade and mineralize CBZ its intermediates following a well-known pathway [62–65]. Because of the good efficiency of compound 2, we have chosen its kinetics to elucidate carbamazepine degradation pathway; table 1 lists possible structures of identified degradation products and their empirical formula and figure 8 illustrate the mechanism of photodegradation. According to radicals formation mechanism; ( $\bullet\text{OH}$ ) and  $\bullet\text{HO}_2$  are the majority radicals present on solution, and are responsible of the degradation of carbamazepine and the formation of photoproducts (Figure 8). Indeed, and as a result of hydroxylation of CBZ an early-stage products P3 and P4 were observed, P3 in its turn gives birth to P7 by epoxy bond cleavage. Thereafter, another hydroxylation takes place to give P2. While the loss of  $-\text{COH}$  and  $-\text{NH}_2$  from P4 structure give birth of P1 and P5 [62]. Another pathway could be proposed for P4 from P3 via rearrangement [62]. Thereafter, hydroxylation of P5 give P6 as a stable product [62,66].



**Figure 4.** Proposed formation mechanism of free hydroxyl radicals by  $(\text{CTA})_4\text{W}_{10}\text{O}_{32}$ .

**Table 1:** Possible structures of identified degradation products and their empirical formula.

Compound	Retention time (min)	[M+H] <sup>+</sup> m/z	Formula	Proposed structure	Ref
CBZ	4.3	237.1025	C <sub>15</sub> H <sub>12</sub> N <sub>2</sub> O		
P1	1.2	224.0706	C <sub>14</sub> H <sub>9</sub> NO <sub>2</sub>		[41]
P2	2.8	271.1077	C <sub>15</sub> H <sub>14</sub> N <sub>2</sub> O <sub>3</sub>		[41,66, 67]
P3	3.06	253.098	C <sub>15</sub> H <sub>12</sub> N <sub>2</sub> O <sub>2</sub>		[67,68]
P4	3.4	253.098	C <sub>15</sub> H <sub>12</sub> N <sub>2</sub> O <sub>2</sub>		[68]
P5	3.4	180.0807	C <sub>13</sub> H <sub>9</sub> N		[41]
P6	3.6	196.0762	C <sub>13</sub> H <sub>9</sub> NO		[41]
P7	4.1	253.098	C <sub>15</sub> H <sub>12</sub> N <sub>2</sub> O <sub>2</sub>		[66,67, 69,70]

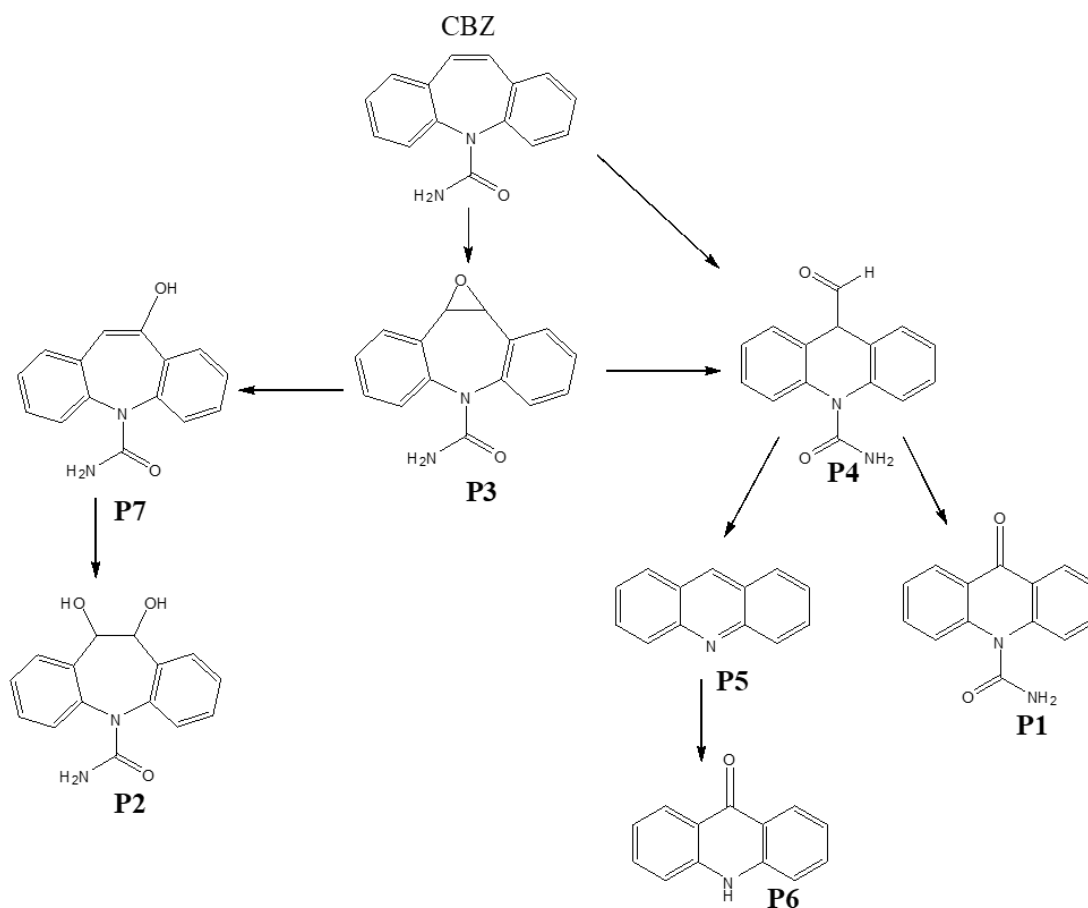


**Figure 8:** Carbamazepine photo-degradation pathway over compound 2 photo-catalyst.

### Leaching Test

The leaching of decatungstate is one of the major drawbacks, which limits the application of the hybrid POM materials. To evidence this process, a simple test was carried out at the end of each photocatalytic experiment. The photocatalyst was filtered from the solution and a drop of ethanol was added to the filtrate and then exposed to UV light. It is well-known that in presence of ethanol and under irradiation, anionic decatungstate ( $W_{10}O_{32}^{4-}$ ) is transformed into reduced decatungstate ( $W_{10}O_{32}^{5-}$ ) characterized by a blue colour as shown for W10 on figure 9 (a). This test allows us to study qualitatively the presence of anionic decatungstate in solution after photocatalytic experiment. In figure 9 (b and c), the absence of a blue colour proved the excellent stability of compounds **1** and **2**.

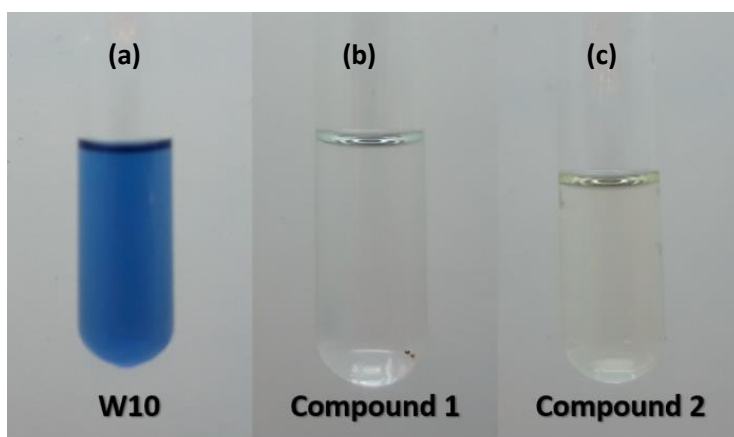


**Figure 9.** Leaching Tests: In leaching case, the filtrate colour must be change to blue indicating characteristic of  $W_{10}O_{32}^{5-}$

## Conclusion

In this study water-insoluble decatungstate based hybrid materials were synthesised in aqueous media by the reaction of decatungstate anion and a hexadecyltrimethylammonium surfactant (CTAB) using different molar ratio (1:1 for compound **1** and 1:3 for compound **2**). TGA and FT-IR spectroscopy reveals the similar elemental composition of both compounds. UV-Visible spectroscopy and SEM shows the different band gap energy (2.42 eV for **1** and 3.02 eV for **2**) and the morphology. These materials are used as a photocatalysts for carbamazepine degradation under UV-visible light irradiation. Both compounds exhibit an interesting photocatalytic activity especially compound **2** and an excellent chemical stability. Using surfactant as heterogenization agent for polyoxometalate appears to be a promising strategy for heterogeneous photocatalysis application.

## References:

- [1] Y. Guo, C. Hu, Heterogeneous photocatalysis by solid polyoxometalates, (2007) 13. [http://files/47/Guo et Hu - 2007 - Heterogeneous photocatalysis by solid polyoxometal.pdf](http://files/47/Guo%20et%20Hu%20-%20Heterogeneous%20photocatalysis%20by%20solid%20polyoxometal.pdf).
- [2] C.L. Hill, Progress and challenges in polyoxometalate-based catalysis and catalytic materials chemistry, (2007) 5. [http://files/44/Hill - 2007 - Progress and challenges in polyoxometalate-based c.pdf](http://files/44/Hill%20-%20Progress%20and%20challenges%20in%20polyoxometalate-based%20c.pdf).
- [3] R. Sivakumar, Polyoxometalate-based molecular/nano composites: Advances in environmental remediation by photocatalysis and biomimetic approaches to solar energy conversion, (2012) 22. [http://files/46/Sivakumar - 2012 - Polyoxometalate-based molecularnano composites A.pdf](http://files/46/Sivakumar%20-%20Polyoxometalate-based%20molecularnano%20composites%20A.pdf).
- [4] C. Streb, New trends in polyoxometalate photoredox chemistry: From photosensitisation to water oxidation catalysis, (2012) 9. [http://files/45/Streb - 2012 - New trends in polyoxometalate photoredox chemistry.pdf](http://files/45/Streb%20-%20New%20trends%20in%20polyoxometalate%20photoredox%20chemistry.pdf).
- [5] S.-S. Wang, G.-Y. Yang, Recent Advances in Polyoxometalate-Catalyzed Reactions, Chem. Rev. (n.d.) 70. [http://files/48/Wang et Yang - Recent Advances in Polyoxometalate-Catalyzed React.pdf](http://files/48/Wang%20et%20Yang%20-%20Recent%20Advances%20in%20Polyoxometalate-Catalyzed%20React.pdf).
- [6] Y. Zhou, Z. Guo, W. Hou, Q. Wang, J. Wang, Polyoxometalate-based phase transfer catalysis for liquid-solid organic reactions: a review, (n.d.) 13. [http://files/43/Zhou et al. - Polyoxometalate-based phase transfer catalysis for.pdf](http://files/43/Zhou%20et%20al.%20-%20Polyoxometalate-based%20phase%20transfer%20catalysis%20for.pdf).
- [7] A. Bijelic, M. Aureliano, A. Rompel, The antibacterial activity of polyoxometalates: Structures, antibiotic effects and future perspectives, Chem. Commun. 54 (2018) 1153–1169. <https://doi.org/10.1039/c7cc07549a>.
- [8] J.T. Rhule, C.L. Hill, D.A. Judd, R.F. Schinazi, Polyoxometalates in Medicine, (n.d.) 32. [http://files/50/Rhule et al. - Polyoxometalates in Medicine.pdf](http://files/50/Rhule%20et%20al.%20-%20Polyoxometalates%20in%20Medicine.pdf).
- [9] M.T. Pope, A. Müller, Polyoxometalate Chemistry: An Old Field with New Dimensions in Several Disciplines, Angew. Chemie Int. Ed. English. 30 (1991) 34–48. <https://doi.org/10.1002/anie.199100341>.
- [10] E. Sousa Da Silva, M. Sarakha, H.D. Burrows, P. Wong-Wah-Chung, Decatungstate anion as an efficient photocatalytic species for the transformation of the pesticide 2-(1-

naphthyl)acetamide in aqueous solution, *J. Photochem. Photobiol. A Chem.* 334 (2017) 61–73. <https://doi.org/10.1016/j.jphotochem.2016.10.036>.

[11] V.I. Supranovich, V. V Levin, A.D. Dilman, Radical Addition to N-Tosylimines via C–H Activation Induced by Decatungstate Photocatalyst, *Org. Lett.* (2019) 4. <http://files/53/Supranovich et al. - 2019 - Radical Addition to N-Tosylimines via C–H Activati.pdf>.

[12] C. Tanielian, Decatungstate photocatalyzed oxygenation of methanol in acetonitrile under photostationary state conditions, (2014) 7. <http://files/210/10.1016@j.jallcom.2020.155669.pdf>.

[13] A. Allaoui, M.A. Malouki, P. Wong-Wah-Chung, Homogeneous photodegradation study of 2-mercaptobenzothiazole photocatalysed by sodium decatungstate salts: Kinetics and mechanistic pathways, *J. Photochem. Photobiol. A Chem.* 212 (2010) 153–160. <https://doi.org/10.1016/j.jphotochem.2010.04.010>.

[14] S. Rafqah, P.W.W. Chung, C. Forano, M. Sarakha, Photocatalytic degradation of metsulfuron methyl in aqueous solution by decatungstate anions, *J. Photochem. Photobiol. A Chem.* 199 (2008) 297–302. <https://doi.org/10.1016/j.jphotochem.2008.06.012>.

[15] I. Texier, C. Giannotti, S. Malato, C. Richter, J. Delaire, Solar photodegradation of pesticides in water by sodium decatungstate, *Catal. Today.* (1999) 11. <http://files/57/Texier et al. - 1999 - Solar photodegradation of pesticides in water by s.pdf>.

[16] B. Orel, U. Lavrenčič-Štangar, M.G. Hutchins, K. Kalcher, Mixed phosphotungstic acid/titanium oxide gels and thin solid xerogel films with electrochromic-ionic conductive properties, *J. Non. Cryst. Solids.* 175 (1994) 251–262. [https://doi.org/10.1016/0022-3093\(94\)90018-3](https://doi.org/10.1016/0022-3093(94)90018-3).

[17] M.C. Pham, M. Mostefai, P.C. Lacaze, Synthesis and characterization of electrodes modified by poly(1-naphthol) films doped with heteropolyanions, *Synth. Met.* 52 (1992) 305–317. [https://doi.org/10.1016/0379-6779\(92\)90030-M](https://doi.org/10.1016/0379-6779(92)90030-M).

[18] S. V. Lomakina, T.S. Shatova, L.P. Kazansky, Heteropoly anions as corrosion inhibitors for aluminium in high temperature water, *Corros. Sci.* 36 (1994) 1645–1651. [https://doi.org/10.1016/0010-938X\(94\)90059-0](https://doi.org/10.1016/0010-938X(94)90059-0).

- [19] O. Oulhakem, H. Zahdi, M. Belaïche, S. Laalioui, Z. Naimi, B. Ikken, K.B. Alaoui, Z. Sekkat, One-step immobilization of tungsten oxide on microporous silica surface as a photocatalyst for water pollutant removal, *Microporous Mesoporous Mater.* 335 (2022) 111784. <https://doi.org/10.1016/j.micromeso.2022.111784>.
- [20] I. Texier, J.A. Delaire, C. Giannotti, Reactivity of the charge transfer excited state of sodium decatungstate at the nanosecond time scale, *Phys. Chem. Chem. Phys.* 2 (2000) 1205–1212. <https://doi.org/10.1039/a908588b>.
- [21] F. Bigi, A. Corradini, C. Quarantelli, G. Sartori, Silica-bound decatungstates as heterogeneous catalysts for H<sub>2</sub>O<sub>2</sub> activation in selective sulfide oxidation, *J. Catal.* 250 (2007) 222–230. <https://doi.org/10.1016/j.jcat.2007.06.019>.
- [22] A. Maldotti, A. Molinari, G. Varani, M. Lenarda, L. Storaro, F. Bigi, R. Maggi, A. Mazzacani, G. Sartori, Immobilization of (n-Bu<sub>4</sub>N)<sub>4</sub>W<sub>10</sub>O<sub>32</sub> on Mesoporous MCM-41 and Amorphous Silicas for Photocatalytic Oxidation of Cycloalkanes with Molecular Oxygen, *J. Catal.* 209 (2002) 210–216. <https://doi.org/10.1006/jcat.2002.3618>.
- [23] A. Molinari, A. Maldotti, A. Bratovic, G. Magnacca, Photocatalytic properties of sodium decatungstate supported on sol–gel silica in the oxidation of glycerol, *Catal. Today*. 206 (2013) 46–52. <https://doi.org/10.1016/j.cattod.2011.11.033>.
- [24] A. Molinari, A. Bratovic, G. Magnacca, A. Maldotti, Matrix effects on the photocatalytic oxidation of alcohols by [nBu<sub>4</sub>N]<sub>4</sub>W<sub>10</sub>O<sub>32</sub> incorporated into sol–gel silica, *Dalt. Trans.* 39 (2010) 7826. <https://doi.org/10.1039/c003282d>.
- [25] A. Molinari, R. Amadelli, A. Mazzacani, G. Sartori, A. Maldotti, Tetralkylammonium and Sodium Decatungstate Heterogenized on Silica: Effects of the Nature of Cations on the Photocatalytic Oxidation of Organic Substrates, (n.d.) 6. <http://files/62/Molinari et al. - Tetralkylammonium and Sodium Decatungstate Heterog.pdf>.
- [26] S. Farhadi, Z. Momeni, Zirconia-supported sodium decatungstate (Na<sub>4</sub>W<sub>10</sub>O<sub>32</sub>/ZrO<sub>2</sub>): An efficient, green and recyclable photocatalyst for selective oxidation of activated alcohols to carbonyl compounds with O<sub>2</sub>, *J. Mol. Catal. A Chem.* 277 (2007) 47–52. <https://doi.org/10.1016/j.molcata.2007.07.024>.
- [27] S. Farhadi, S. Sepahvand, Na<sub>4</sub>W<sub>10</sub>O<sub>32</sub>/ZrO<sub>2</sub> nanocomposite prepared via a sol-gel route: A novel, green and recoverable photocatalyst for reductive cleavage of

408 azobenzenes to amines with 2-propanol, *J. Mol. Catal. A Chem.* 318 (2010) 75–84.  
 409 <https://doi.org/10.1016/j.molcata.2009.11.010>.

410 [28] L. Li, Y. Yang, R. Fan, J. Liu, Y. Jiang, B. Yang, W. Cao, Decatungstate acid improves  
 411 the photo-induced electron lifetime and retards the recombination in dye sensitized  
 412 solar cells, *Dalt. Trans.* 45 (2016) 14940–14947. <https://doi.org/10.1039/C6DT02584F>.

413 [29] M.D. Tzirakis, I.N. Lykakis, G.D. Panagiotou, K. Bourikas, A. Lycourghiotis, C.  
 414 Kordulis, M. Orfanopoulos, Decatungstate catalyst supported on silica and  $\gamma$ -alumina:  
 415 Efficient photocatalytic oxidation of benzyl alcohols, *J. Catal.* (2007) 12.  
 416 [http://files/65/Tzirakis et al. - 2007 - Decatungstate catalyst supported on silica and  \$\gamma\$  -  
 417 .pdf](http://files/65/Tzirakis et al. - 2007 - Decatungstate catalyst supported on silica and \gamma - .pdf).

418 [30] X. Yang, F. Qian, Y. Wang, M. Li, J. Lu, Y. Li, M. Bao, Constructing a novel ternary  
 419 composite (C16H33(CH3)3N)4W10O32/g-C3N4/rGO with enhanced visible-light-  
 420 driven photocatalytic activity for degradation of dyes and phenol, *Appl. Catal. B*  
 421 *Environ.* 200 (2017) 283–296. <https://doi.org/10.1016/j.apcatb.2016.07.024>.

422 [31] A. Misra, K. Kozma, C. Streb, M. Nyman, Beyond Charge Balance: Counter-Cations  
 423 in Polyoxometalate Chemistry, *Angew. Chemie - Int. Ed.* 59 (2020) 596–612.  
 424 <https://doi.org/10.1002/anie.201905600>.

425 [32] T. Ito, T. Yamase, Controllable Layered Structures in Polyoxomolybdate-Surfactant  
 426 Hybrid Crystals, *Materials (Basel)*. 3 (2010) 158–164.  
 427 <https://doi.org/10.3390/ma3010158>.

428 [33] M. Nyman, M.A. Rodriguez, T.M. Anderson, D. Ingersoll, Two Structures Toward  
 429 Understanding Evolution from Surfactant-Polyoxometalate Lamellae to Surfactant-  
 430 Encapsulated Polyoxometalates, *Cryst. Growth Des.* 9 (2009) 3590–3597.  
 431 <https://doi.org/10.1021/cg9003356>.

432 [34] M. Nyman, D. Ingersoll, S. Singh, F. Bonhomme, T.M. Alam, C.J. Brinker, M.A.  
 433 Rodriguez, Comparative Study of Inorganic Cluster-Surfactant Arrays, (n.d.) 11.  
 434 <http://files/19/Nyman et al. - Comparative Study of Inorganic Cluster-Surfactant .pdf>.

435 [35] B. Ohtani, Preparing Articles on Photocatalysis—Beyond the Illusions,  
 436 Misconceptions, and Speculation, *Chem. Lett.* 37 (2008) 216–229.  
 437 <https://doi.org/10.1246/cl.2008.216>.

- 438 [36] X. Yan, T. Ohno, K. Nishijima, R. Abe, B. Ohtani, Is methylene blue an appropriate  
439 substrate for a photocatalytic activity test? A study with visible-light responsive titania,  
440 Chem. Phys. Lett. (2006) 5. [http://files/168/\[Pure and Applied Chemistry\]](http://files/168/[Pure and Applied Chemistry])  
441 Physisorption of gases with special reference to the evaluation of surface area and pore  
442 size distribution (IUPAC Technical Report).pdf.
- 443 [37] R. Andreozzi, M. Raffaele, Pharmaceuticals in STP effluents and their solar  
444 photodegradation in aquatic environment, (2003) 12. <http://files/15/Andreozzi et>  
445 Raffaele - 2003 - Pharmaceuticals in STP effluents and their solar pho.pdf.
- 446 [38] P. Falås, H.R. Andersen, A. Ledin, Occurrence and reduction of pharmaceuticals in the  
447 water phase at Swedish wastewater treatment plants, Water Sci. (2012) 10.  
448 <http://files/13/Falås et al. - 2012 - Occurrence and reduction of pharmaceuticals in>  
449 the.pdf.
- 450 [39] C.D. Metcalfe, X.-S. Miao, B.G. Koenig, J. Struger, Distribution of acidic and neutral  
451 drugs in surface waters near sewage treatment plants in the lower Great Lakes, Canada,  
452 (n.d.) 9. <http://files/14/Metcalfe et al. - Distribution of acidic and neutral drugs in>  
453 surfac.pdf.
- 454 [40] P.E. Stackelberg, J. Gibbs, E.T. Furlong, M.T. Meyer, S.D. Zaugg, R.L. Lippincott,  
455 Efficiency of conventional drinking-water-treatment processes in removal of  
456 pharmaceuticals and other organic compounds, Sci. Total Environ. (2007) 18.  
457 <http://files/198/duan2019.pdf>.
- 458 [41] R. Meribout, Y. Zuo, A.A. Khodja, A. Piram, S. Lebarillier, J. Cheng, C. Wang, P.  
459 Wong-Wah-Chung, Photocatalytic degradation of antiepileptic drug carbamazepine  
460 with bismuth oxychlorides (BiOCl and BiOCl/AgCl composite) in water: Efficiency  
461 evaluation and elucidation degradation pathways, J. Photochem. Photobiol. A Chem.  
462 328 (2016) 105–113. <https://doi.org/10.1016/j.jphotochem.2016.04.024>.
- 463 [42] O.Y. Poimanova, S. V Radio, K.Y. Bilousova, V.N. Baumer, G.M. Rozantsev,  
464 Equilibria in the acidified aqueous-dimethylformamide solutions of tungstate-anion.  
465 Synthesis, crystal structure and characterization of decatungstate, (n.d.) 33.  
466 <http://files/25/Poimanova et al. - Equilibria in the acidified aqueous->  
467 dimethylformam.pdf.
- 468 [43] O.Y. Poimanova, S. V Radio, K.Y. Bilousova, D. V Khaustov, V.N. Baumer, G.M.

Rozantsev, Phase formation in the system  $\text{Co}^{2+} - \text{WO}_4^{2-} - \text{H}^+ - \text{C}_3\text{H}_7\text{ON} - \text{H}_2\text{O}$ .  
 Synthesis, crystal structure and characterization of cobalt(II) decatungstate, (n.d.) 25.  
[http://files/26/Poimanova et al. - Phase formation in the system  \$\text{Co}^{2+} - \text{WO}\_4^{2-} - \text{H}^+ -\$](http://files/26/Poimanova et al. - Phase formation in the system Co2+ - WO42- - H+ - .pdf)   
[.pdf](http://files/26/Poimanova et al. - Phase formation in the system Co2+ - WO42- - H+ - .pdf).

[44] R.B. Viana, Infrared Spectroscopy of Anionic, Cationic, and Zwitterionic Surfactants,  
 Adv. Phys. Chem. (n.d.) 15. [http://files/27/Viana - Infrared Spectroscopy of Anionic,](http://files/27/Viana - Infrared Spectroscopy of Anionic, Cationic, and Zw.pdf)  
[Cationic, and Zw.pdf](http://files/27/Viana - Infrared Spectroscopy of Anionic, Cationic, and Zw.pdf).

[45] V. Kulikov, G. Meyer, Organoamine silver( I ) decatungstate structures: remarkable  
 chemoselectivity and the exploration of the intramolecular redox reaction upon  
 thermolysis, New J. Chem. 38 (2014) 3408. <https://doi.org/10.1039/C4NJ00172A>.

[46] S. Wang, S. Xing, Z. Shi, J. He, Q. Han, M. Li, Electrostatic polypyridine–ruthenium(  
 II )···decatungstate dyads: structures, characterizations and photodegradation of dye,  
 RSC Adv. 7 (2017) 18024–18031. <https://doi.org/10.1039/C7RA01342F>.

[47] V. Kulikov, G. Meyer, Polyoxotungstates in Molecular Boxes of Purine Bases, (2014)  
 10. [http://files/23/Kulikov et Meyer - 2014 - Polyoxotungstates in Molecular Boxes of](http://files/23/Kulikov et Meyer - 2014 - Polyoxotungstates in Molecular Boxes of Purine Bas.pdf)  
[Purine Bas.pdf](http://files/23/Kulikov et Meyer - 2014 - Polyoxotungstates in Molecular Boxes of Purine Bas.pdf).

[48] M. Avila, L. Reguera, J. Rodríguez-Hernández, J. Balmaseda, E. Reguera, Porous  
 framework of  $\text{T}_2[\text{Fe}(\text{CN})_6] \cdot x\text{H}_2\text{O}$  with  $\text{T}=\text{Co}, \text{Ni}, \text{Cu}, \text{Zn}$ , and  $\text{H}_2$  storage, J. Solid  
 State Chem. 181 (2008) 2899–2907. <https://doi.org/10.1016/j.jssc.2008.07.030>.

[49] X.H. Liu, X.H. Luo, S.X. Lu, J.C. Zhang, W.L. Cao, A novel cetyltrimethyl  
 ammonium silver bromide complex and silver bromide nanoparticles obtained by the  
 surfactant counterion, J. Colloid Interface Sci. 307 (2007) 94–100.  
<https://doi.org/10.1016/j.jcis.2006.11.051>.

[50] Z. Sui, X. Chen, L. Wang, Y. Chai, C. Yang, J. Zhao, An improved approach for  
 synthesis of positively charged silver nanoparticles, Chem. Lett. 34 (2005) 100–101.  
<https://doi.org/10.1246/cl.2005.100>.

[51] Z.M. Sui, X. Chen, L.Y. Wang, L.M. Xu, W.C. Zhuang, Y.C. Chai, C.J. Yang,  
 Capping effect of CTAB on positively charged Ag nanoparticles, Phys. E Low-  
 Dimensional Syst. Nanostructures. 33 (2006) 308–314.  
<https://doi.org/10.1016/j.physe.2006.03.151>.

- 499 [52] J.M. Salazar, G. Weber, J.M. Simon, I. Bezverkhyy, J.P. Bellat, Characterization of  
500 adsorbed water in MIL-53(Al) by FTIR spectroscopy and ab-initio calculations, *J.*  
501 *Chem. Phys.* 142 (2015). <https://doi.org/10.1063/1.4914903>.
- 502 [53] S.H. Wu, D.H. Chen, Synthesis of high-concentration Cu nanoparticles in aqueous  
503 CTAB solutions, *J. Colloid Interface Sci.* 273 (2004) 165–169.  
504 <https://doi.org/10.1016/j.jcis.2004.01.071>.
- 505 [54] A.T. Shah, A. Mujahid, M.U. Farooq, W. Ahmad, B. Li, M. Irfan, M.A. Qadir, Micelle  
506 directed synthesis of (C<sub>19</sub>H<sub>42</sub>N)<sub>4</sub>H<sub>3</sub>(PW<sub>11</sub>O<sub>39</sub>) nanoparticles and their catalytic  
507 efficiency for oxidative degradation of azo dye, *J. Sol-Gel Sci. Technol.* 63 (2012)  
508 194–199. <https://doi.org/10.1007/s10971-012-2779-6>.
- 509 [55] L. Wei, Z. Ming, Z. Jinli, H. Yongcai, Self-assembly of cetyl trimethylammonium  
510 bromide in ethanol-water mixtures, (n.d.) 5. [http://files/28/Wei et al. - Self-assembly of](http://files/28/Wei%20et%20al.%20-%20Self-assembly%20of%20cetyl%20trimethylammonium%20bromide%20i.pdf)  
511 [cetyl trimethylammonium bromide i.pdf](http://files/28/Wei%20et%20al.%20-%20Self-assembly%20of%20cetyl%20trimethylammonium%20bromide%20i.pdf).
- 512 [56] D. Ravelli, D. Dondi, M. Fagnoni, A. Albini, A. Bagnoli, Electronic and EPR spectra of  
513 the species involved in [W<sub>10</sub>O<sub>32</sub>]<sup>4-</sup> photocatalysis. A relativistic DFT investigation,  
514 *Phys. Chem. Chem. Phys.* 15 (2013) 2890. <https://doi.org/10.1039/c2cp43950f>.
- 515 [57] Z. Chen, H.N. Dinh, E. Miller, Photoelectrochemical water splitting: standards,  
516 experimental methods, and protocols, Springer, New York, 2013. [http://files/30/Chen](http://files/30/Chen%20et%20al.%20-%202013%20-%20Photoelectrochemical%20water%20splitting%20standards%20e.pdf)  
517 [et al. - 2013 - Photoelectrochemical water splitting standards, e.pdf](http://files/30/Chen%20et%20al.%20-%202013%20-%20Photoelectrochemical%20water%20splitting%20standards%20e.pdf).
- 518 [58] X. Zhao, S. Zhang, J. Yan, L. Li, G. Wu, W. Shi, G. Yang, N. Guan, P. Cheng,  
519 Polyoxometalate-Based Metal–Organic Frameworks as Visible-Light-Induced  
520 Photocatalysts, *Inorg. Chem.* (2018) 8. [http://files/33/Zhao et al. - 2018 -](http://files/33/Zhao%20et%20al.%20-%202018%20-%20Polyoxometalate-Based%20Metal-Organic%20Frameworks%20as.pdf)  
521 [Polyoxometalate-Based Metal–Organic Frameworks as .pdf](http://files/33/Zhao%20et%20al.%20-%202018%20-%20Polyoxometalate-Based%20Metal-Organic%20Frameworks%20as.pdf).
- 522 [59] J.T. Jasper, D.L. Sedlak, Phototransformation of Wastewater-Derived Trace Organic  
523 Contaminants in Open-Water Unit Process Treatment Wetlands, *Environ. Sci.* (n.d.)  
524 10. [http://files/34/Jasper et Sedlak - Phototransformation of Wastewater-Derived Trace](http://files/34/Jasper%20et%20Sedlak%20-%20Phototransformation%20of%20Wastewater-Derived%20Trace%20Organic.pdf)  
525 [Or.pdf](http://files/34/Jasper%20et%20Sedlak%20-%20Phototransformation%20of%20Wastewater-Derived%20Trace%20Organic.pdf).
- 526 [60] D.C. Duncan, T.L. Netzel, C.L. Hill, Early-Time Dynamics and Reactivity of  
527 Polyoxometalate Excited States. Identification of a Short-Lived LMCT Excited State  
528 and a Reactive Long-Lived Charge-Transfer Intermediate following Picosecond Flash  
529 Excitation of [W<sub>10</sub>O<sub>32</sub>]<sup>4-</sup> in Acetonitrile, *Inorg. Chem.* 34 (1995) 4640–4646.

<https://doi.org/10.1021/ic00122a021>.

- [61] A. Molinari, R. Argazzi, A. Maldotti, Photocatalysis with Na<sub>4</sub>W<sub>10</sub>O<sub>32</sub> in water system: Formation and reactivity of OH radicals, *J. Mol. Catal. A Chem.* 372 (2013) 23–28. <https://doi.org/10.1016/j.molcata.2013.01.037>.
- [62] Y. Duan, Assembly of graphene on Ag<sub>3</sub>PO<sub>4</sub>/AgI for effective degradation of carbamazepine under Visible-light irradiation: Mechanism and degradation pathways, (n.d.) 37. [http://files/38/Duan - Assembly of graphene on Ag<sub>3</sub>PO<sub>4</sub>AgI for effective d.pdf](http://files/38/Duan - Assembly of graphene on Ag3PO4AgI for effective d.pdf).
- [63] Z. Hu, X. Cai, Z. Wang, S. Li, Z. Wang, X. Xie, Construction of carbon-doped supramolecule-based g-C<sub>3</sub>N<sub>4</sub>/TiO<sub>2</sub> composites T for removal of diclofenac and carbamazepine: A comparative study of operating parameters, mechanisms, degradation pathways, *J. Hazard. Mater.* (2019) 14. <http://files/39/Hu et al. - 2019 - Construction of carbon-doped supramolecule-based g.pdf>.
- [64] S. Li, Z. Wang, X. Zhao, X. Yang, G. Liang, X. Xie, Insight into enhanced carbamazepine photodegradation over biochar-based magnetic photocatalyst Fe<sub>3</sub>O<sub>4</sub>/BiOBr/BC under visible LED light irradiation, *Chem. Eng. J.* 360 (2019) 600–611. <https://doi.org/10.1016/j.cej.2018.12.002>.
- [65] M. Moztahida, J. Jang, M. Nawaz, S.-R. Lim, D.S. Lee, Effect of rGO loading on Fe<sub>3</sub>O<sub>4</sub>: A visible light assisted catalyst material for carbamazepine degradation, *Sci. Total Environ.* (2019) 10. [http://files/40/Moztahida et al. - 2019 - Effect of rGO loading on Fe<sub>3</sub>O<sub>4</sub> A visible light as.pdf](http://files/40/Moztahida et al. - 2019 - Effect of rGO loading on Fe3O4 A visible light as.pdf).
- [66] Y. Hong, H. Zhou, Z. Xiong, Y. Liu, G. Yao, B. Lai, Heterogeneous activation of peroxymonosulfate by CoMgFe-LDO for degradation of carbamazepine: Efficiency, mechanism and degradation pathways, *Chem. Eng. J.* (2019) 123604. <https://doi.org/10.1016/j.cej.2019.123604>.
- [67] M. Nawaz, W. Miran, J. Jang, D.S. Lee, One-step hydrothermal synthesis of porous 3D reduced graphene oxide/TiO<sub>2</sub> aerogel for carbamazepine photodegradation in aqueous solution, *Appl. Catal. B Environ.* 203 (2017) 85–95. <https://doi.org/10.1016/j.apcatb.2016.10.007>.
- [68] A.B. Martínez-Piernas, S. Nahim-Granados, M.I. Polo-López, P. Fernández-Ibáñez, S. Murgolo, G. Mascolo, A. Agüera, Identification of transformation products of

carbamazepine in lettuce crops irrigated with Ultraviolet-C treated water, *Environ. Pollut.* 247 (2019) 1009–1019. <https://doi.org/10.1016/j.envpol.2019.02.001>.

[69] C. Tanielian, K. Duffy, A. Jones, Kinetic and Mechanistic Aspects of Photocatalysis by Polyoxotungstates: A Laser Flash Photolysis, Pulse Radiolysis, and Continuous Photolysis Study, (n.d.) 7. <http://files/41/Tanielian et al. - Kinetic and Mechanistic Aspects of Photocatalysis .pdf>.

[70] V. De Waele, O. Poizat, M. Fagnoni, A. Bagnò, D. Ravelli, Unraveling the Key Features of the Reactive State of Decatungstate Anion in Hydrogen Atom Transfer (HAT) Photocatalysis, *ACS Catal.* (2016) 9. <http://files/42/Waele et al. - 2016 - Unraveling the Key Features of the Reactive State .pdf>.